

Theory of the Elasto-Optic Effect in Nonmetallic Crystals

S. H. WEMPLE AND M. DiDOMENICO, JR.

Bell Telephone Laboratories, Murray Hill, New Jersey 07974

(Received 14 July 1969; revised manuscript received 15 September 1969)

General expressions are derived for the magnitude and dispersion of elasto-optic coefficients in terms of strain-induced modifications of both the electronic energy-band structure, and, if present, the excitonic structure. This analysis uses the deformation potential concept in conjunction with oscillator models for the important optical transitions to describe strain-induced energy shifts, and also emphasizes the importance of strain-dependent oscillator strengths. Results are compared with existing elasto-optic dispersion data in materials having no excitonic contribution (e.g., LiNbO₃ and Si) and in materials with important excitonic contributions (e.g., alkali halides and CdS). In the case of ferroelectric crystals, two important ferroelectricity-related contributions to the elasto-optic effect are identified. The first relates to a strain-dependent Curie temperature, and the second to the enhancing effect of polarization fluctuations near the Curie point in the paraelectric phase.

I. INTRODUCTION

A SIMPLE oscillator model for the electro-optic and nonlinear optic effects in solids has recently been applied successfully to the class of oxygen-octahedra ferroelectrics.¹ This model approximates the energy-band structure with physically meaningful oscillators, and then describes refractive index variations in terms of energy shifts and strength changes of these oscillators. As shown in Ref. 1, the connection between refractive-index variations and perturbations in oscillator parameters is more generally useful than had been thought previously, because one of the important parameters required to make this connection turns out to have nearly the same numerical value in many, if not most, crystalline solids. The purpose of this paper is to extend the analysis of Ref. 1 to the elasto-optic (photo-elastic) effect. As in the electro-optic and nonlinear optic cases, we define useful phenomenological parameters which are closely related to fundamental microscopic quantities, i.e., we introduce a deformation potential \mathfrak{D} to describe energy shifts and a dispersion parameter \mathcal{K} to describe strength changes. In terms of these two parameters, general expressions are derived for the magnitude and dispersion of the elasto-optic p coefficients. Our analysis includes both interband and exciton transitions and shows that crystals having strong excitonic bands (e.g., CdS, ZnO, and the alkali halides) can be expected to exhibit anomalously strong dispersion in the p coefficients. Finally, we consider the special case of ferroelectric crystals and find that strain-induced changes in the Curie point can give rise to a large elasto-optic contribution in the ferroelectric phase. This contribution, as we shall show, is equivalent to the electro-optic contribution expected in piezoelectric crystals. In ferroelectric crystals we also propose that due to the presence of strain-dependent polarization fluctuations, an unexpectedly large enhancement of the

elasto-optic coefficients occurs on cooling toward the Curie point in the paraelectric phase.

In order to describe the elasto-optic effect we use the usual definitions and relate the optical impermeability (inverse dielectric constant) to the strain tensor x_{ij} through a fourth-rank elasto-optic p tensor. To be more general, we also include a possible electro-optic contribution and use the polarization P_k as the driving term rather than the electric field. The impermeability change is then given in terms of the elasto-optic p coefficients and electro-optic f coefficients by the expression

$$\Delta\left(\frac{1}{n^2}\right)_{ij} = \sum_{k,l} p_{ijkl}^P x_{kl} + \sum_k f_{ijk}^x P_k, \quad (1)$$

where the superscripts x and P denote that these coefficients are measured at constant strain and constant polarization, respectively. The conditions of measurement are important in piezoelectric crystals where the applied strain produces an induced polarization. For this reason, a distinction should be made between coefficients measured at constant polarization (p^P) and those measured at constant field (p^E). It can be shown that these quantities are related by

$$p_{ijkl}^E - p_{ijkl}^P = \sum_m f_{ijm}^x e_{mkl}^E, \quad (2)$$

where the piezoelectric e coefficients are defined by²

$$P_k = \sum_{l,m} e_{klm}^E x_{lm}. \quad (3)$$

II. CALCULATION OF INTERBAND CONTRIBUTION TO ELASTO-OPTIC COEFFICIENTS

A. Energy-Band Formulation

A formal procedure for calculation of the elasto-optic coefficients is contained in the band theory of

¹ M. DiDomenico, Jr., and S. H. Wemple, *J. Appl. Phys.* **40**, 720 (1969); S. H. Wemple and M. DiDomenico, Jr., *ibid.* **40**, 735 (1969).

² The superscript E on e^E serves to distinguish this quantity from its value measured at constant displacement e^D . We point out also that $p^E \approx p^D$ in ferroelectric materials.

solids. In principle, the imaginary part of the dielectric response function $\epsilon_{ij} = \epsilon_{1,ij} + i\epsilon_{2,ij}$ can be computed from a knowledge of the band structure and the one-electron wave functions. The real part in the region of transparency is then given by the Kramers-Kronig (KK) integral

$$\epsilon_{1,ij}(\omega) - 1 = \frac{2}{\pi} \int_{\omega_g}^{\infty} \frac{\omega' \epsilon_{2,ij}(\omega')}{(\omega'^2 - \omega^2)} d\omega'. \quad (4)$$

Here ω_g refers to the absorption threshold frequency. In the presence of strain, the wave functions and energy bands will be modified slightly. From Eq. (4), changes in ϵ_1 and ϵ_2 are related by

$$\Delta \epsilon_{1,ij}(\omega) = - \frac{2}{\pi} \int_{\omega_g'}^{\infty} \frac{\omega' \Delta \epsilon_{2,ij}(\omega')}{(\omega'^2 - \omega^2)} d\omega', \quad (5)$$

where $\omega_g' = \omega_g + \Delta\omega_g$, and $\Delta\omega_g$ is the strain-induced shift in the absorption threshold. The quantity $\Delta\epsilon_1$ in Eq. (5) is related to the impermeability $\Delta(1/\epsilon_1) = \Delta(1/n^2)$ by the expression¹

$$\Delta \epsilon_{1,ij} = - \sum_{k,l} \epsilon_{1,ik} \Delta(1/\epsilon_1)_{kl} \epsilon_{1,lj}. \quad (6)$$

Substituting Eq. (1) into this relation in the limit where $P=0$ and making use of Eq. (5), we obtain a formal relationship between the elasto-optic p^P coefficients and the strain-induced changes in the interband absorption spectrum, i.e.,

$$\sum_{k,l,m,n} \epsilon_{1,ik} \epsilon_{1,lj} p_{klmn}^P x_{mn} = - \frac{2}{\pi} \int_{\omega_g'}^{\infty} \frac{\omega' \Delta \epsilon_{2,ij}^P(\omega')}{(\omega'^2 - \omega^2)} d\omega'. \quad (7)$$

A similar expression holds for p^E . In the following presentation we omit the superscripts for clarity.

To proceed further, we can either attempt the difficult task of calculating $\Delta \epsilon_{2,ij}$ for each strain component x_{mn} , or we can resort to models which contain physically useful experimental parameters. In this paper, we adopt the latter point of view and use phenomenological parameters in simple oscillator approximations³ to Eqs. (4) and (5). There is a third alternative which is to make use of the classical Clausius-Mossotti model of a solid with polarizable point ions as has been done in detail by Mueller⁴ for cubic crystals. In this model, local-field corrections and ionic polarizabilities are introduced to circumvent the more complex energy-band problem. Because no allowance is made for covalency and because ionic polarizabilities appear to be meaningful parameters only in the alkali halides,⁵ we feel that such a description is of limited usefulness.

³ More complicated and consequently less useful oscillator descriptions have been used previously in the analysis of elasto-optic data. See, S. Ramaseshan and V. Swaramakrishnan, *Current Sci. (India)* **25**, 246 (1956).

⁴ H. Mueller, *Phys. Rev.* **47**, 947 (1935).

⁵ A. H. Kahn, J. A. Tesson, and W. Shockley, *Phys. Rev.* **92**, 890 (1953).

B. Simplified Oscillator Formulation

It has been shown experimentally^{1,6} that the interband contributions to ϵ_1 can be accurately fitted to a single-oscillator Sellmeier expression in the over 50 widely different *ionic* and *covalent* crystals for which reliable refractive-index dispersion data are available. This remarkable result is found⁶ to apply with high accuracy in compounds having the diamond, zincblende, wurtzite, rocksalt, CsCl, and CaF₂ structures as well as in a variety of complex oxides. Thus, for an arbitrary light-polarization direction (denoted by the superscript σ) the wavelength dependence of ϵ_1^σ is given closely by the relation

$$\epsilon_1^\sigma(\lambda) - 1 = S_0^\sigma (\lambda_0^\sigma)^2 [1 - (\lambda_0^\sigma/\lambda)^2]^{-1}. \quad (8)$$

Here λ is the light wavelength and S_0^σ and λ_0^σ are oscillator strength and position parameters, respectively. As discussed in Ref. 6, Eq. (8) is not only valid experimentally but the interband energy ($\mathcal{E}_0 = hc/e\lambda_0$) and interband strength [$\mathcal{F} = (hc/e)^2 S_0$] parameters are physically meaningful (h is Planck's constant, c is the speed of light, and e is the electronic charge). Using these parameters we can define a "dispersion energy" \mathcal{E}_d given by $\mathcal{E}_d \equiv \mathcal{F}/\mathcal{E}_0 = (hc/e) S_0 \lambda_0$. The dispersion energy determines the dispersion of the electronic dielectric constant in nonmetallic nonmagnetic solids, and has been shown⁶ to obey an extraordinarily simple empirical relation involving crystal structure, chemical valency, and ground-state electronic configuration.

We can view Eq. (8) as a long-wavelength approximation to the KK integral given by Eq. (4). It is easy to show⁶ using the KK expression that the average interband oscillator strength \mathcal{F}^σ and the average interband oscillator position \mathcal{E}_0^σ are given by the following *moment integrals* of the fundamental ϵ_2 spectrum:

$$(\mathcal{E}_0^\sigma)^2 = \left(\frac{h}{e}\right)^2 \int_{\omega_g}^{\infty} \frac{\epsilon_2^\sigma}{\omega} d\omega / \int_{\omega_g}^{\infty} \frac{\epsilon_2^\sigma}{\omega^3} d\omega, \quad (9)$$

$$\mathcal{F}^\sigma = \frac{2}{\pi} \left(\frac{h}{e}\right)^2 \left(\int_{\omega_g}^{\infty} \frac{\epsilon_2^\sigma}{\omega} d\omega \right)^2 / \int_{\omega_g}^{\infty} \frac{\epsilon_2^\sigma}{\omega^3} d\omega. \quad (10)$$

It is clear from Eqs. (9) and (10) that the ϵ_2 spectrum is weighted most heavily towards the band edge. In the immediate vicinity of the band edge, however, the value of ϵ_2 drops rapidly to zero, so that the band edge itself should not be considered a contributor to either the refractive index or its dispersion. We can show further, using a known relationship between absorption and the refractive index [see Eq. (22)], that optical absorptions above the band edge contribute very little to the refractive index until the absorption coefficient approaches 10^5 cm^{-1} . Thus direct transitions near the band edge have a very small influence on re-

⁶ S. H. Wemple and M. DiDomenico, Jr., *Phys. Rev. Letters* **23**, 1156 (1969).

fractive-index behavior below the band edge, and indirect transitions can be entirely neglected. It is for this reason that Eq. (8) continues to be a good approximation for optical wavelengths quite close to the band edge. It should also be noted that the Sellmeier parameters expressed by Eq. (9) and (10) are related to moment integrals over *all* interband absorptions and are entirely independent of the optical wavelength. An exception to the above arguments occurs if one or more strong exciton bands (peak absorption coefficient of approximately 10^6 cm^{-1}) are present just below the interband edge. In this case Eq. (8) will continue to be valid at long wavelengths, but for wavelengths approaching the exciton absorption deviations will occur as discussed in Sec. IV. Even when excitons are present, however, the exciton contribution to the long-wavelength refractive index is quite small.

In terms of our single-oscillator model, crystal strain induces changes in oscillator position $\Delta \mathcal{E}_0^\sigma$ and strength $\Delta \mathcal{F}^\sigma$. These quantities, which are related to integrals over the $\epsilon_2^\sigma(\omega)$ and $\Delta \epsilon_2^\sigma(\omega)$ spectra, can be computed using Eqs. (9) and (10). From Eq. (8) we find that the strain-induced change in ϵ_1^σ is given by

$$\Delta \epsilon_1^\sigma / (\epsilon_1^\sigma - 1)^2 = -2(\Delta \mathcal{E}_0^\sigma / \mathcal{E}_d^\sigma) \{1 + K^\sigma [1 - (\lambda_0^\sigma / \lambda)^2]\}, \quad (11)$$

where

$$K^\sigma = -\frac{1}{2} \left(\frac{\Delta \mathcal{F}^\sigma / \mathcal{F}^\sigma}{\Delta \mathcal{E}_0^\sigma / \mathcal{E}_0^\sigma} \right) \quad (12)$$

and $\mathcal{E}_d^\sigma = \mathcal{F}^\sigma / \mathcal{E}_0^\sigma = (hc/e) S_0^\sigma \lambda_0^\sigma$ is the dispersion energy defined above. We now introduce a deformation potential parameter D_{ij}^σ which relates the oscillator shift $\Delta \mathcal{E}_0^\sigma$ to the strain components x_{ij} , i.e.,

$$\Delta \mathcal{E}_0^\sigma = \sum_{i,j} D_{ij}^\sigma x_{ij}. \quad (13)$$

The deformation potential does not apply to any specific interband transition but involves all transitions integrated throughout the Brillouin zone that contribute to $\epsilon_2^\sigma(\omega)$. We anticipate, however, that its order of magnitude can be estimated from shifts in the band gap with strain, typically several eV. Equation (11) provides a useful framework on which to build a full tensor description of the elasto-optic effect in optically anisotropic crystals provided that the quantities ϵ_1^σ , \mathcal{E}_d^σ , and \mathcal{E}_0^σ (or λ_0^σ) are *approximately isotropic*. We thus define an "average" impermeability $1/\epsilon_1$ and an "average" oscillator position \mathcal{E}_0 where the average is taken, for example, over the values appropriate to the principal dielectric axes of an anisotropic crystal. We also make use of the experimental result^{1,6} that in many anisotropic crystals the quantity \mathcal{E}_d is not only very nearly isotropic but also has a *unique* value which depends in a simple way on the anion valency and crystal structure (see below).

Incorporating the above approximations into Eqs. (1), (6), and (11) we find that

$$\frac{p_{ij}^\sigma}{(1-1/n^2)^2} = \frac{2}{\mathcal{E}_d} D_{ij}^\sigma \left[1 + K^\sigma \left(1 - \frac{\lambda_0^{\sigma 2}}{\lambda^2} \right) \right]. \quad (14)$$

In Eq. (14), p_{ij}^σ is the elasto-optic coefficient for light polarized along the σ axis when strain component x_{ij} is applied. It is thus *not* one of the tensor elements. The subscripts merely indicate the associated strain component. Since only two direction-dependent parameters D_{ij}^σ and K^σ are required to describe the complete direction dependence of the elasto-optic effect, we now generalize Eq. (14) to apply to each fourth-rank tensor component p_{ijkl} by redefining the deformation potential D_{ij}^σ and the constant K^σ in terms of new phenomenological fourth-rank tensor parameters \mathcal{D}_{ijkl} and \mathcal{K}_{ijkl} . In standard reduced index notation, the tensor result is

$$\frac{p_{ij}}{(1-1/n^2)^2} = \frac{2}{\mathcal{E}_d} \mathcal{D}_{ij} \left[1 + \mathcal{K}_{ij} \left(1 - \frac{\lambda_0^2}{\lambda^2} \right) \right], \quad (15)$$

where \mathcal{D}_{ij} and \mathcal{K}_{ij} can be measured experimentally in crystals obeying the isotropy conditions given above. We emphasize that each of the \mathcal{D}_{ij} and \mathcal{K}_{ij} tensor components can be expressed in terms of $\epsilon_{2,ij}$ and $\Delta \epsilon_{2,ij}$ and thus can be related directly to the energy-band structure.

Our final result [Eq. (15)] can be viewed as a two-parameter fit to elasto-optic dispersion data. The parameters \mathcal{E}_0 (or λ_0) and \mathcal{E}_d can be obtained separately from refractive-index dispersion measurements.⁶ It is clear from the form of Eq. (15) that the dispersion of the p coefficients, or more precisely

$$\frac{p}{(1-1/n^2)^2},$$

is determined by the parameter \mathcal{K} . In the simplest case where only a single band shifts in energy but not in strength we have $\mathcal{K}=0$, and this quantity is dispersionless. More generally $\mathcal{K} \neq 0$ either because several bands shift in energy (but not necessarily strength) by different amounts, or because the strengths of the transitions are strain-dependent. Both alternatives lead to dispersion in

$$\frac{p}{(1-1/n^2)^2}.$$

The dispersion of a particular p coefficient may be either positive or negative depending on the sign and magnitude of \mathcal{K} . For $-1 < \mathcal{K} < 0$, the dispersion is positive, i.e., p increases on approaching the absorption edge, whereas for $\mathcal{K} > 0$ or $\mathcal{K} < -1$ the dispersion is negative. Whether a positive or negative dispersion

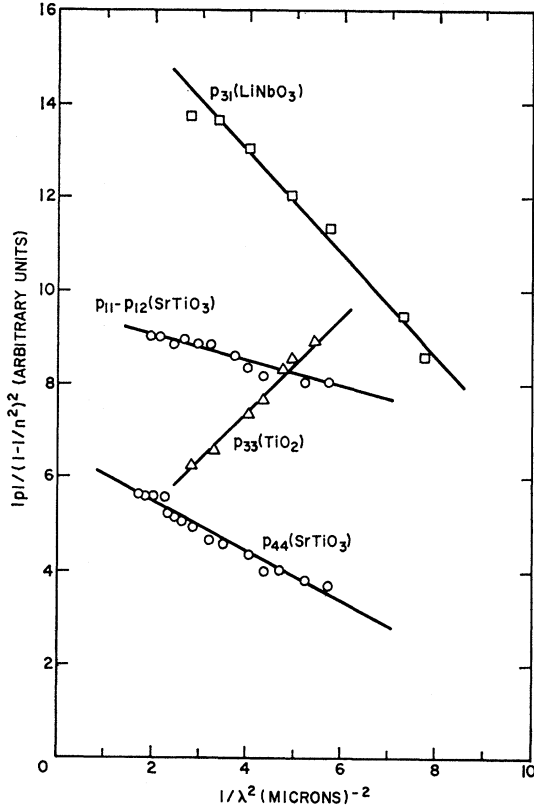


FIG. 1. Dispersion of elasto-optic coefficients in LiNbO_3 , SrTiO_3 , and TiO_2 at room temperature.

occurs depends on the precise nature of strain-induced energy-band changes and is not necessarily indicative of differences in the physical mechanism.

As pointed out above, the dispersion energy \mathcal{E}_d has been found empirically to have nearly the same value in many crystalline solids^{1,6} when proper account is taken of the valency of the anion element and crystal structure. We now make use of this observation to simplify Eq. (15). Detailed discussions of the quantity \mathcal{E}_d are given elsewhere⁶; here we merely quote the final result, viz.,

$$\mathcal{E}_d = \beta N_c Z_a N_e, \quad (16)$$

where N_c is the nearest-neighbor cation coordination number, Z_a is the formal anion valency, and N_e is the effective number of valence electrons per anion. The constant β can assume two values: $\beta_i \approx 0.26$ eV in ionic compounds and $\beta_c \approx 0.39$ eV in covalent compounds. Substituting Eq. (16) into Eq. (15) yields

$$\frac{p_{ij}}{(1-1/n^2)^2} = \frac{2}{\beta N_c Z_a N_e} \mathcal{D}_{ij} \left[1 + \mathcal{K}_{ij} \left(1 - \frac{\lambda_0^2}{\lambda^2} \right) \right]. \quad (17)$$

Equation (17) can be used to estimate the magnitude of the interband contribution to the p coefficients in

solids. Taking, for example, $Z_a=2$, $N_c=6$, $N_e=8$, $\beta_i=0.26$ eV, $n=2$, and $\mathcal{K}=0$, we find for $\lambda \gg \lambda_0$ that $p \sim 0.05\mathcal{D}$. Since deformation potentials are expected to be a few eV, we conclude that $p \sim 0.1$ which is the correct order of magnitude.

Before proceeding further, it is useful to ask what Eq. (15) implies in terms of a microscopic model of the elasto-optic effect. We noted previously that this equation gives a simple two-parameter formulation of the magnitude and dispersion of the elasto-optic coefficients in solids. Superficially, these parameters, the deformation potential \mathcal{D} and the dispersion constant \mathcal{K} , appear to be wholly phenomenological and unrelated to identifiable microscopic interactions. The apparent reason is that precise calculations require complete knowledge of $\epsilon_2(\omega)$ and $\Delta\epsilon_2(\omega)$. This, in turn, means that the complete energy-band structure is known, and, in particular, how each level shifts in energy throughout the entire Brillouin zone as a function of strain. In our approach we have avoided this difficult (and usually unsolved) problem by resorting to a physically meaningful Sellmeier oscillator description of the index of refraction, and further have introduced a deformation potential parameter to describe strain-induced shifts in the average Sellmeier oscillator position and strength. This approach is not only a useful parametrization of the elasto-optic problem, but is also significant from the standpoint of microscopic interactions. The reason is that the deformation potential can be estimated, in the tight-binding approximation, from the strain-induced modifications in the energy-overlap integrals between the basic molecular orbitals describing the valence and conduction-band states.

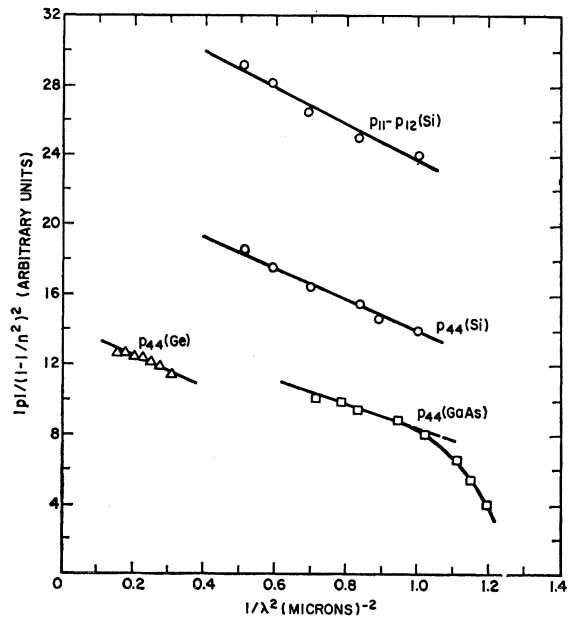


FIG. 2. Dispersion of elasto-optic coefficients in GaAs, Ge, and Si.

III. COMPARISON WITH EXPERIMENT

Comparison of the wavelength dispersion predicted by Eqs. (15) and (17) with experiment can be made on only a few materials since dispersion data are very limited. In Figs. 1-3 we have plotted representative elasto-optic dispersion data taken from various sources⁷⁻¹³ for different types of materials. All the data, with the exception of LiNbO₃ and TiO₂, were obtained from static stress-optical experiments. The LiNbO₃ and TiO₂ data were obtained by Dixon⁷ using ultrasonic light-scattering techniques.¹⁴ In plotting the

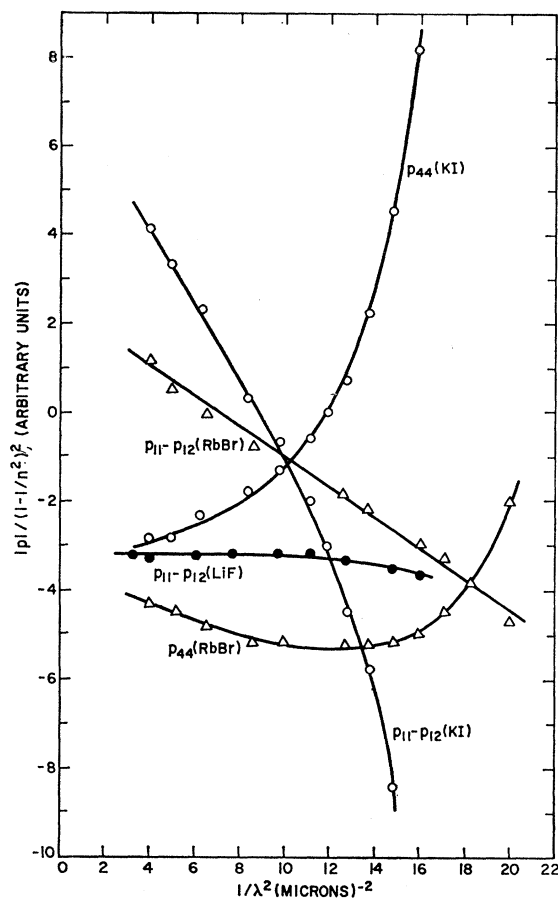


FIG. 3. Dispersion of elasto-optic coefficients in KI, RbBr, and LiF.

- ⁷ R. W. Dixon (unpublished results); LiNbO₃ and TiO₂.
⁸ A. A. Giardini, *J. Opt. Soc. Am.* **47**, 726 (1957); SrTiO₃.
⁹ V. I. Nikitenko and G. P. Martynenko, *Fiz. Tverd. Tela* **7**, 622 (1965) [English transl.: *Soviet Phys.—Solid State* **7**, 494 (1965)]; Si.
¹⁰ A. Feldman and D. Horowitz, Jr., *J. Appl. Phys.* **39**, 5597 (1968); GaAs.
¹¹ A. Feldman, *Phys. Rev.* **150**, 748 (1966); Ge.
¹² A. Gavini and M. Cardona, *Phys. Rev.* **177**, 1351 (1969); KI and RbBr.
¹³ R. Srinivasan, *Naturwiss.* **48**, 96 (1961); LiF.

TABLE I. Some representative values of \mathcal{D} and \mathcal{K} extracted from Figs. 1 and 2.

Material	ρ Coefficient	\mathcal{D} (eV)	\mathcal{K}	ϵ_0 (eV) ^a
SrTiO ₃ ^b	ρ_{44}	0.7	-2.2	5.74
LiNbO ₃ ^c	ρ_{31}	-4	-2	7.08, 6.74
TiO ₂ ^c	ρ_{33}	3.6	-0.9	5.26, 5.17
Si ^d	ρ_{44}	-4.7	-1.3	4.0

- ^a See Ref. 6.
^b See Ref. 8.
^c R. W. Dixon (unpublished results).
^d See Ref. 9.

quantity

$$\frac{|\rho|}{(1 - 1/n^2)^2}$$

versus $1/\lambda^2$ in Figs. 1-3, we have, for convenience, used arbitrary scales for the ordinate.

Apart from GaAs and the alkali halides near their interband edges, the dispersion data shown in Figs. 1-3 fit Eq. (15) reasonably well. Because of the difficulty in estimating errors in elasto-optic experiments it is not possible at the present time to draw hard conclusions as to the general validity of Eq. (15). More elasto-optic dispersion data are needed; however, the results presented in Figs. 1-3 suggest that Eq. (15) may provide a sound basis for data analysis in many materials. The increased dispersion in GaAs and the alkali halides near the interband edge shown in Figs. 2 and 3 implies that the single effective interband-oscillator model is not applicable to these materials. Strong transitions near the band edge are clearly important. As discussed in Sec. IV, strain-dependent excitonic transitions can lead to substantial increases in the elasto-optic dispersion on approaching the interband edge without strongly affecting the refractive-index dispersion.

For those materials which obey Eq. (15) we can estimate the parameters \mathcal{D} and \mathcal{K} from the magnitude and dispersion of the ρ coefficients. Some representative results are listed in Table I. As expected, \mathcal{D} values are of the order of an eV, and $|\mathcal{K}|$ does not differ substantially from 1. It is of interest to note that all the listed \mathcal{K} values are negative indicating that strain-induced shifts in oscillator energy and strength have the same sign in all these materials [see Eq. (12)]. We point out also that the value of \mathcal{K} obtained from elasto-optic data may be quite different from that obtained from other kinds of experiments. For example, the dispersion of the static birefringence in LiNbO₃¹ is described by $\mathcal{K} \approx 0$ rather than $\mathcal{K} \approx -2$. This result is not surprising in view of the expected difference between strain-induced and polarization-induced energy-band distortions.

¹⁴ R. W. Dixon and M. G. Cohen, *Appl. Phys. Letters* **8**, 205 (1966).

IV. CONTRIBUTION OF EXCITONS TO ELASTO-OPTIC COEFFICIENTS

Equation (4) applies, in general, whatever the source of $\epsilon_{2,ij}$. When excitons are present, one or more strong-absorption peaks appear slightly below the fundamental absorption edge. Strain-induced shifts, splittings, and strength changes of these bands are thus expected to alter the refractive index and contribute to the elasto-optic coefficients. Furthermore, we would expect anomalously strong-wavelength dispersion of this excitonic contribution because of the close proximity of the exciton bands to the region of transparency. Gavini and Cardona¹² have, in fact, evaluated exciton deformation potentials in several alkali halides using elasto-optic dispersion data (see below for a discussion of their results).

Just as in the interband case presented in Sec. II we approximate the exciton contribution to the refractive index n by a single effective oscillator. In the low-absorption range we then obtain

$$n^2 - 1 = \frac{S_e \lambda_e^2}{(1 - \lambda_e^2/\lambda^2)} + \frac{S_0 \lambda_0^2}{(1 - \lambda_0^2/\lambda^2)}, \quad (18)$$

where the first term gives the excitonic contribution (transition strength S_e and oscillator position λ_e), and the second term gives the interband contribution discussed in Sec. II. Tensor notation has been deleted for clarity. Considering only the strain-induced changes in the exciton band, we find on differentiating Eq. (18) that

$$\Delta n^2 = -2(\Delta \mathcal{E}_e/\mathcal{E}_e) \chi_e (1 - \lambda_e^2/\lambda^2)^{-2} \times [1 + K_e (1 - \lambda_e^2/\lambda^2)], \quad (19)$$

where

$$K_e = -\frac{1}{2} \left(\frac{\Delta S_e/S_e}{\Delta \mathcal{E}_e/\mathcal{E}_e} \right) \quad (20)$$

and χ_e refers to the exciton band contribution to the long-wavelength optical susceptibility given by $S_e \lambda_e^2$. Using the definition of the p coefficients given earlier and relating $\Delta \mathcal{E}_e$ to strain through an excitonic deformation potential D_e , Eq. (19) becomes

$$p_e = 2(\chi_e/n_0^4)(D_e/\mathcal{E}_e)(1 - \lambda_e^2/\lambda^2)^{-2} \times [1 + K_e(1 - \lambda_e^2/\lambda^2)]. \quad (21)$$

Equation (21) gives the elasto-optic coefficient associated with an exciton band located at energy \mathcal{E}_e . We can compare the magnitude of p_e with the interband part p_0 given by Eq. (15) by estimating the magnitude of χ_e from the following expression¹⁵ for the excitonic

¹⁵ See, for example, T. S. Moss, *Optical Properties of Semiconductors* (Butterworth Scientific Publications Ltd., London, 1961), p. 27. The total refractive index is given by $n = 1 + (1/2\pi^2) \int_0^\infty \alpha d\lambda$, where 1 refers to the vacuum contribution, and α is the total absorption coefficient from all sources.

contribution n_e to the total long-wavelength refractive index $n = n_0 + n_e$:

$$n_e = (1/2\pi^2) \int_{\Delta \lambda_e} \alpha_e d\lambda, \quad (22)$$

where α_e is the exciton absorption coefficient, and the integral extends over the exciton band of interest. For an order-of-magnitude estimate we take¹⁶ $\alpha_e \approx 10^6 \text{ cm}^{-1}$ and $\Delta \lambda_e \approx 100 \text{ \AA}$. Equation (22) then yields $n_e \sim 0.05$. The susceptibility χ_e is given by $n^2 - n_0^2$, from which we obtain $\chi_e \approx 2n_0 n_e \sim 0.2$ for $n_e \ll n_0$ (n_0 is the background interband contribution). For definiteness we assume further that $D_e \sim 1 \text{ eV}$, $K_e \approx 0$,¹⁷ $n_0 \approx 2$, and $\mathcal{E}_e \approx 4 \text{ eV}$. Substitution into Eq. (21) then yields $p_e \sim 0.006$ for $\lambda \gg \lambda_e$. This value compares with $p_0 \sim 0.1$ previously estimated for the interband contribution. We note, however, that p_e exhibits a very strong wavelength dispersion and that p_e increases markedly as λ approaches λ_e , while at the same time p_0 remains relatively constant. For example, at $\lambda = 1.1\lambda_e$ we find that $p_e \sim 0.1$ which is comparable to p_0 .

We now turn to the dispersion predicted by Eq. (11). To facilitate comparison with published data, we compute the logarithmic slope $d(\ln p_e)/d(\ln \lambda)$ given by

$$d(\ln p_e)/d(\ln \lambda) \approx -4[(\lambda/\lambda_e)^2 - 1]^{-1}, \quad (23)$$

where we have neglected dispersion in n_0 and have assumed that $K_e = 0$. It is of interest to compare this result with the interband expression obtained from Eq. (15), i.e.,

$$d(\ln p_0)/d(\ln \lambda) \approx 2[(1 + 1/3\epsilon)(\lambda^2/\lambda_0^2) - 1]^{-1}, \quad (24)$$

where, consistent with Eq. (23), the dispersion in n_0 has been neglected. Since $\lambda_e > \lambda_0$ and $\lambda > \lambda_e$, the exciton contribution, if present, always dominates the interband contribution near the band edge. Direct comparison of Eq. (23) with experiment can be made using the results of Tell *et al.*¹⁸ on CdS and ZnO. These authors find very strong dispersion in the p_{12} and p_{31} coefficients and considerably weaker dispersion in p_{11} . The observed dispersion in p_{12} and p_{31} is much too large to be accounted for by the interband contribution given by Eq. (24). For CdS, Tell *et al.* find for both p_{12} and p_{31} that $d(\ln p)/d(\ln \lambda) \approx -10$, while for ZnO they find $d(\ln p)/d(\ln \lambda) \approx -4$ with p_{31} exhibiting slightly stronger dispersion than p_{12} . By taking $\lambda_e \approx 0.5 \mu$ ¹⁹ and $\lambda = 0.575 \mu$ for CdS, we predict from Eq. (23) that $d(\ln p)/d(\ln \lambda) \approx -12$ in agreement with experiment. A similar conclusion holds for ZnO. Strain-induced shifts in the

¹⁶ H. R. Philipp and H. Ehrenreich, *Phys. Rev.* **131**, 2016 (1963).

¹⁷ This value of K_e assumes a simple exciton band shift without changes in strength (i.e., $\Delta S_e = 0$).

¹⁸ B. Tell, J. M. Worlock, and L. J. Martin, *Appl. Phys. Letters* **6**, 123 (1965).

¹⁹ J. E. Rowe, M. Cardona, and F. H. Pollack, in *II-VI Semiconducting Compounds*, edited by D. G. Thomas (W. A. Benjamin, Inc., New York, 1967), p. 112.

exciton bands can thus account for the anomalously strong dispersion observed in CdS and ZnO.

Increased dispersion observed in the alkali halides near the interband edge (see Fig. 3) is also very probably due to excitons. Gavini and Cardona¹² drew this same conclusion and estimated values of exciton deformation potentials in several alkali halides using elasto-optic dispersion data. These authors, however, did not consider the possible interband contribution to the total observed dispersion. According to our model, elasto-optic data should be fitted to the sum of Eqs. (15) and (21), whereas Gavini and Cardona used an expression corresponding to Eq. (21) alone. In our model, the nonmonotonic behavior of p_{44} in RbBr observed by these authors can be understood in terms of a dominant excitonic contribution at short wavelengths and a dominant interband contribution at long wavelengths. For illustrative purposes we can use the long-wavelength data together with Eq. (17) with $Z_a=1$, $N_c=6$, $N_v=8$, and $\beta=0.26$ eV to estimate \mathcal{D}_{44} and \mathcal{K}_{44} in RbBr. The results are $\mathcal{D}_{44}\approx -0.5$ eV and $\mathcal{K}_{44}\approx -0.7$.

To summarize, our deformation potential model of the elasto-optic effect provides a two-parameter fit to the interband contribution which agrees with experiment in several materials in which excitons are absent. Both of these parameters are found to have "reasonable" values. In the more general case involving excitons a four-parameter fit is required to describe the complete dispersion data. We have not attempted detailed fits to published data, however, simply because an ample number of fitting parameters is clearly at our disposal.

V. SPECIAL EFFECTS IN FERROELECTRIC CRYSTALS

Although the discussion up to this point should be applicable to any crystalline solid, there are special features in ferroelectric crystals which require separate examination. We consider here additional contributions to the elasto-optic coefficients present in the ferroelectric and paraelectric phase which are uniquely associated with the occurrence of ferroelectricity.

A. Ferroelectric Phase

In piezoelectric crystals, where applied strain produces lattice polarization, it is important to distinguish between elasto-optic measurements made at constant field p^E and at constant polarization p^P [see Eq. (2)]. The reason, of course, is that the strain-induced polarization can produce a refractive-index variation via the electro-optic effect. The basic lattice contribution to the elasto-optic effect is described by p^P and is expected to follow Eq. (15). The p^E coefficient is the superposition of the basic p^P coefficient and the additional strain-induced electro-optic effect. In ferroelectric crystals

this latter effect can be quite large and in fact exceed the basic p^P contribution.

The spontaneous polarization P_s of a ferroelectric is a function of the temperature difference $T_c - T$, where T_c is the Curie point. Since the refractive index depends on the magnitude of P_s , strain-induced shifts in the Curie point will modify the refractive index. This Curie-point shift is the origin of the strain-induced electro-optic contribution to the p^E elasto-optic coefficients and can be calculated quite generally for the class of oxygen-octahedra ferroelectrics.²⁰ These materials include, for example, perovskite (e.g., BaTiO₃), tungsten bronze (e.g., Ba₂NaNb₅O₁₅), and LiNbO₃-type structures. In order to make a connection between the Curie point and the refractive index, we first relate the spontaneous polarization P_s to the refractive index. As described in detail in Ref. 1 polarization-induced refractive index changes in the ferroelectric phase can be written in terms of the *quadratic* electro-optic g coefficients associated with the centro-symmetric paraelectric phase. These electro-optic g coefficients are defined by the relation

$$\Delta\left(\frac{1}{n^2}\right)_{ij} = \sum_{k,l} g_{ijkl} P_k P_l, \quad (25)$$

where P_k refers to the k th component of the *total* crystal polarization. An important simplification occurs in oxygen-octahedra ferroelectrics where the g -tensor elements are found to have the same *numerical* magnitude when expressed in a coordinate system aligned along principal axes of the basic BO₆ octahedron building block.¹ The orthogonal transformations that relate these fundamental g coefficients to the g coefficients in Eq. (25), appropriate to the principal axes of the spontaneously polarized crystal, are given elsewhere.¹

In a strained crystal, Eq. (25) must be modified to include the basic elasto-optic contribution p^P associated with crystal strain. The result is

$$\Delta\left(\frac{1}{n^2}\right)_{ij} = \sum_{k,l} (g_{ijkl}^x P_k P_l + p_{ijkl}^P x_{kl}). \quad (26)$$

Here, as before, the superscripts x and P denote measurements at constant strain and constant polarization, respectively. The strain components in Eq. (26) include both polarization-induced (electrostriction) and stress-induced contributions. An incremental change in strain δx_{mn} modifies Eq. (26) to read

$$\frac{\delta[\Delta(1/n^2)_{ij}]}{\delta x_{mn}} = 2 \sum_k g_{ijk^3}^x P_k \frac{\delta P_k}{\delta x_{mn}} + \sum_{k,l} p_{ijkl}^P \frac{\delta x_{kl}}{\delta x_{mn}}, \quad (27)$$

where the spontaneous polarization axis has been taken

²⁰ See Ref. 1 for a discussion of these materials and their structure.

to be the 3 axis. For elasto-optic measurements at constant electric field Eq. (27) gives

$$p_{ijmn}^E = g_{ij33}^X \frac{\delta P_s^2}{\delta x_{mn}} + 2 \sum_{k \neq 3} g_{ijk3}^X P_s \frac{\delta P_k}{\delta x_{mn}} + \sum_{k,l} p_{ijkl}^P \frac{\delta x_{kl}}{\delta x_{mn}}. \quad (28)$$

This equation is identical to Eq. (2) when we recognize that $2gP_s$ gives the electro-optic f tensor (see Ref. 1 for details) and that $e^E = \delta P / \delta x$. Equation (28) can be further simplified by introducing electrostriction explicitly, i.e.,

$$x_{kl} = x_{kl}^P + \sum_{u,v} Q_{kluv}^X P_u P_v, \quad (29)$$

where the electrostriction Q tensor is defined at constant stress as indicated by the superscript X . Substituting the derivative of Eq. (29) with respect to strain into Eq. (28), we obtain

$$p_{ijmn}^E = g_{ij33}^X \frac{\delta P_s^2}{\delta x_{mn}} + 2 \sum_{k \neq 3} g_{ijk3}^X P_s e_{kmn}^E + \sum_{k,l} p_{ijkl}^P \frac{\delta x_{kl}^P}{\delta x_{mn}}, \quad (30)$$

where

$$g_{ijkl}^X = g_{ijkl}^x + \sum_{m,n} p_{ijmn}^P Q_{mnkl}^X \quad (31)$$

and

$$e_{kmn}^E = \delta P_k / \delta x_{mn}. \quad (32)$$

The third term in Eq. (30) gives the direct strain effect resulting from the change in unit-cell volume and is not related to the ferroelectricity, while the first two terms give the electro-optic contribution associated with the piezoelectric effect. We have explicitly shown the strain-dependent spontaneous polarization contribution in the first term, i.e.,

$$\hat{p}_{ijmn} = g_{ij33}^X (\delta P_s^2 / \delta x_{mn}).$$

We can compute the magnitude of \hat{p}_{ijmn} under the assumption that it is caused by a strain-dependent Curie temperature. This assumption is equivalent to our use of the following simplified one-dimensional free-energy expression:

$$F = \frac{1}{2} [(T - T_0^x) / \epsilon_0 C] P^2 + \frac{1}{4} \xi^x P^4 + \frac{1}{6} \eta^x P^6 + \frac{1}{2} c^P x^2 - q x P^2, \quad (33)$$

where ϵ_0 is the free-space permittivity, $q = Q^X c^P$, c^P is the elastic constant, C is the Curie constant, T_0^x is the constant-strain Curie-Weiss temperature, and ξ^x and η^x are assumed temperature-independent coefficients at zero strain. By combining the first and last terms we observe that the electrostrictive effect is equivalent

to a strain-dependent Curie-Weiss temperature, i.e., $T_0 = T_0^x + 2\epsilon_0 C c^P Q^X x$. Since all other coefficients are assumed to be independent of both temperature and strain, the strain-induced spontaneous-polarization change derived from Eq. (33) is related only to the strain-dependent Curie-Weiss temperature. Using this thermodynamic treatment it can be shown¹ that

$$\delta P_s^2 / \delta T_0 = 2\kappa_c P_s^2 / C, \quad (34)$$

where κ_c is the static relative dielectric constant along the spontaneous polarization or c axis. The strain-dependent spontaneous polarization contribution to p^E is then simply

$$\hat{p}_{ijmn} = 2g_{ij33}^X (\kappa_c P_s^2 / C) (\delta T_0 / \delta x_{mn}). \quad (35)$$

To give a numerical example, we make use of the observation that the hydrostatic-pressure variation of T_0 in several perovskite ferroelectrics is approximately $-5^\circ\text{C}/\text{kbar}$ from which we estimate $|\delta T_0 / \delta x| \approx 10^{10} \text{C}$ using a typical bulk modulus of $2 \times 10^3 \text{ kbar}$. Taking $g \approx 0.1 \text{ m}^4 / \text{C}^2$ and $C \approx 1.5 \times 10^{10} \text{ C}^1$ we find on substitution into Eq. (35) that $\hat{p} \approx \kappa_c P_s^2 / 100$. Since $\kappa_c P_s^2$ varies between 10 and 100 in a wide range of oxygen-octahedra ferroelectrics,¹ we predict a very large contribution to the elasto-optic effect, viz., $\hat{p} \approx 0.1 - 1$.

It is of interest to compare in detail the above model with the observed hydrostatic-pressure dependence of the refractive indices in LiNbO_3 reported by Vedam and Davis.²¹ Since no shear strain components along principal axes are present in such experiments, Eq. (30) is simplified considerably. Taking the crystal point-group symmetry to be $3m$ below T_0 and $\bar{3}m$ above T_0 we then find, for example, that

$$\Delta p_{11} = g_{13} (\delta P_s^2 / \delta x_1) - 2g_{14} e_{22}^E P_s, \\ \Delta p_{33} = g_{33} (\delta P_s^2 / \delta x_3), \quad \text{etc.},$$

where $\Delta p = p^E - p^P$. A further simplification occurs in LiNbO_3 because structurally this material has approximately $6mm$ symmetry though the actual point-group symmetry is $3m$. This comes about because the NbO_6 octahedra stacked along the threefold P_s axis are alternately rotated by very nearly 180° .¹ Because g_{14} and e_{22} are identically zero in $6mm$ symmetry, we expect that terms containing the products of these quantities will be small in LiNbO_3 . A consequence of this observation is that only the strain dependence of P_s is important in the hydrostatic-pressure experiments. As a result, the total p^E coefficient is then given by Eq. (35) plus the direct strain contribution given by the p^P term in Eq. (30). In order to compare our Curie-temperature-shift model with the hydrostatic-pressure results, it is convenient to recast the analysis in terms of hydrostatic stress X_0 , since we have a reasonable estimate for

²¹ K. Vedam and T. A. Davis, Appl. Phys. Letters 12, 138 (1968).

$\delta T_0/\delta X_0$ of $-5^\circ\text{C}/\text{kbar}$. The Curie-temperature-shift contributions to $\delta n_3/\delta X_0$ and $\delta n_1/\delta X_0$ are obtained from Eq. (35) by replacing x by X . We then find

$$\delta n_3/\delta X_0 = n_3^3 g_{33} (-\delta T_0/\delta X_0) (\kappa_c P_s^2/C) \quad (36)$$

and

$$\delta n_1/\delta X_0 = n_1^3 g_{13} (-\delta T_0/\delta X_0) (\kappa_c P_s^2/C). \quad (37)$$

Taking

$$\begin{aligned} n_1 &= 2.299, & n_3 &= 2.210, & g_{13} &\approx 0.03 m^4/C^2, \\ g_{33} &\approx 0.1 m^4/C^2, & C &\approx 1.5 \times 10^5 \text{ }^\circ\text{C}, & \kappa_c P_s^2 &= 15 \end{aligned}$$

(see Ref. 1 for numerical values), and $\delta T_0/\delta X_0 \approx -5^\circ\text{C}/\text{kbar}$, we obtain $\delta n_3/\delta X_0 \approx 6 \times 10^{-4} \text{ kbar}^{-1}$ and $\delta n_1/\delta X_0 \approx 2 \times 10^{-4} \text{ kbar}^{-1}$. The values measured by Vedam and Davis²¹ are $\delta \eta_3/\delta X_0 = 6.9 \times 10^{-4} \text{ kbar}^{-1}$ and $\delta n_1/\delta X_0 = 3.2 \times 10^{-4} \text{ kbar}^{-1}$. The agreement between experimental results and our Curie-temperature-shift model implies that the quantity $\delta T_0/\delta X_0$, which has not to our knowledge been measured in LiNbO_3 , has very nearly the same value as in other oxide ferroelectrics, viz., $-5^\circ\text{C}/\text{kbar}$. Finally, since the computed value of $\delta n/\delta X_0$, which neglects the p^P contribution, agrees with experiment we conclude that the p^P contribution may be of order $10^{-4} \text{ kbar}^{-1}$.

B. Paraelectric Phase

The foregoing discussion has assumed that all measurements were performed in the ferroelectric phase where $P_s \neq 0$. We now ask if the elasto-optic properties exhibit any special ferroelectricity-related behavior in the paraelectric phase. Experimental data are severely limited in this temperature range. Measurements of $p_{11} - p_{12}$ and p_{44} in the cubic phase of $\text{KTa}_{0.65}\text{Nb}_{0.35}\text{O}_3$ performed by Price²² show that these coefficients increase by almost a factor of 2 on cooling towards T_c ($\approx 0^\circ\text{C}$). We now propose a physical model to account for such behavior. We postulate that the refractive index can be separated into two contributions. The first and major contribution n_0 is spatially uniform and is unrelated to ferroelectricity. It seems from interband transitions. The second contribution δn is related directly to the presence of random lattice-polarization fluctuations which, in high-dielectric-constant materials, have appreciable mean-square amplitude.

The index of refraction of the medium can be written as

$$n = n_0 + \langle \delta n \rangle, \quad (38)$$

where $\langle \delta n \rangle$ denotes the space-time average macroscopic index fluctuation. This quantity is related to the mean-square polarization fluctuation $\langle \delta P^2 \rangle$ via an average quadratic electro-optic coefficient $\langle g \rangle$, i.e.,

$$\langle \delta n \rangle = -(\frac{1}{2} n_0^3) \langle g \rangle \langle \delta P^2 \rangle. \quad (39)$$

²² E. E. Price (unpublished results).

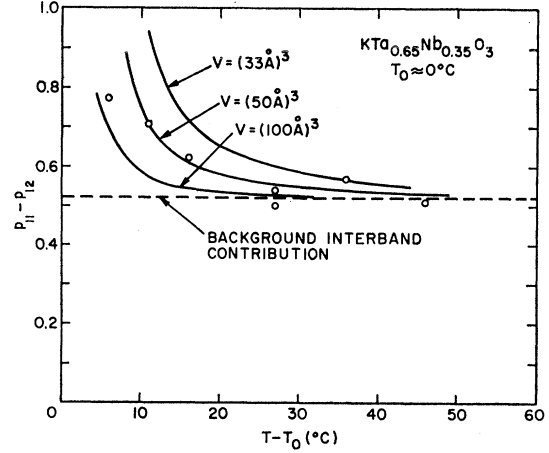


FIG. 4. Temperature dependence of $p_{11} - p_{12}$ in $\text{KTa}_{0.65}\text{Nb}_{0.35}\text{O}_3$. The fluctuation-theory contribution has been calculated from Eq. (43) with $T_0 = 0^\circ\text{C}$, and $V = (33 \text{ \AA})^3$, $(50 \text{ \AA})^3$, and $(100 \text{ \AA})^3$.

The quantity $\langle \delta P^2 \rangle$ can be calculated from the fluctuation dissipation theorem^{23,24} which gives

$$\langle \delta P^2 \rangle = kT \epsilon^x / V, \quad (40)$$

where kT is the thermal energy, ϵ^x is the clamped low-frequency dielectric constant, and V is a characteristic volume corresponding approximately to the size of a polarization-fluctuation cluster.^{24,25} Substituting Eqs. (39) and (40) into (38) and differentiating with respect to strain, we find that

$$p = p_0 + (\langle g \rangle kT / V) (\delta \epsilon^x / \delta x), \quad (41)$$

where p_0 is the background interband contribution. Taking $\epsilon^x = \epsilon_0 C / (T - T_0)$, we then obtain

$$p = p_0 + (\langle g \rangle \epsilon_0 C k / V) [T / (T - T_0)^2] (\delta T_0 / \delta x). \quad (42)$$

If we neglect the temperature dependence of V , Eq. (42) predicts that the elasto-optic coefficients should increase as $T / (T - T_0)^2$ on cooling toward the Curie point. Precise conclusions regarding the magnitude of the fluctuation contribution cannot be made because the ratio $\langle g \rangle / V$ as well as its temperature dependence are unknown. However, an estimate can be made using the following reasonable values for the parameters^{1,25}: $\langle g \rangle \approx 0.1 m^4/C^2$, $C \approx 10^5 \text{ }^\circ\text{C}$, and $|\delta T_0 / \delta x| \approx 10^4 \text{ }^\circ\text{C}$. Using these values we estimate that

$$|p - p_0| \approx (10^4 / V) [T / (T - T_0)^2], \quad (43)$$

where V is the correlation volume in \AA^3 . In Fig. 4, we

²³ *Fluctuation Phenomena in Solids*, edited by R. E. Burgess (Academic Press Inc., New York, 1965).

²⁴ M. DiDomenico, Jr., S. H. Wemple, S. P. S. Porto, and R. P. Bauman, *Phys. Rev.* **174**, 522 (1968).

²⁵ S. H. Wemple, M. DiDomenico, Jr., and A. Jayaraman, *Phys. Rev.* **180**, 547 (1969).

show the temperature dependence of $p_{11}-p_{12}$ as measured by Price²² in $\text{KTa}_{0.65}\text{Nb}_{0.35}\text{O}_3$ ($T_0 \approx 0^\circ\text{C}$) together with our predictions for $V = (33 \text{ \AA})^3$, $(50 \text{ \AA})^3$, and $(100 \text{ \AA})^3$. It is clear that the experimental results are consistent with a "reasonable" correlation volume of $(50 \text{ \AA})^3$ (e.g., see Ref. 25). More precise conclusions must await further experimental observations in a wider range of ferroelectric materials.

Note added in proof. Recent ultrasonic measurements of the temperature dependence of p_{11} and p_{12} in the paraelectric phase of BaTiO_3 [M. G. Cohen, M. DiDomenico, Jr., and S. H. Wemple, Phys. Rev. (to be published)] confirm the validity of Eq. (42) and lend strong support to the view that the correlation volume V is at most a weak function of temperature and does not display critical behavior in displacive ferroelectrics. These measurements give a value $V \approx 4.5 \times 10^5 \text{ \AA}^3$ for BaTiO_3 .

VI. CONCLUSIONS

By combining a physically meaningful Sellmeier-oscillator description of the optical susceptibility with appropriately defined strain-induced changes, we have derived a phenomenological expression for the magnitude and dispersion of the elasto-optic tensor coeffi-

cients. According to our model the microscopic origin of the elasto-optic effect is in strain-induced modifications of the electronic energy-band structure. As a consequence, the p coefficients are found to be directly proportional to a deformation potential parameter; a similar result was found previously¹ for the electro-optic effect where the deformation potential is replaced by the polarization potential. In addition to the basic interband contribution to the elasto-optic coefficients, we have also calculated the influence of excitons, and have shown that excitonic effects become dominant under conditions where the exciton absorption is strong and the exciton transition energy is sensitive to strain. In the case of ferroelectric crystals two important elasto-optic contributions have been identified. The first relates to the effect of strain-induced Curie-point shifts in the ferroelectric phase, and the second to the enhancing effect of polarization fluctuations near the Curie point in the paraelectric phase.

ACKNOWLEDGMENTS

We wish to thank M. G. Cohen for his comments on the manuscript. We also wish to express our thanks to R. W. Dixon for kindly making available to us unpublished elasto-optic data for LiNbO_3 and TiO_2 .